Design and optimization of a full band fiber optic light source

Xubo Dong [1], Jiaye Fang [2] and Siqi Wang [3, *]

[1] School of Physics and Electronic Information, Henan Polytechnic University, Henan, China

[2] International Education College, Changchun Institute of Technology, Changchun, China

[3] School of Optical-Electrical and Computer Engineering, University of Shanghai for Science and Technology, Shanghai, China

* Corresponding author: 2012140119@st.usst.edu.cn

Abstract. In this paper, we study and select the optical fiber materials, and fluorotellurite was finally chosen as the substrate material and co-doped with appropriate amounts of praseodymium ions (Pr^{3+}) and erbium ions (Er^{3+}), to achieve full-bandwidth luminescence of praseodymium and erbium co-doped fluorotellurite glasses pumped by a laser with a wavelength of 488 nm in the range of 1300 nm to 1680 nm, which includes all optical bands from O- to L-bands. In addition, the optical fiber amplifier's working principle is described in terms of the four- and three-energy level systems for praseodymium and erbium ions, respectively, and the rate and power propagation equations in the steady state are established to analyze the influences of the fiber length, the doping concentration, and the pump power on the fiber-optic amplifier gain, which are optimized using a simulated annealing algorithm. A novel amplifier design strategy is presented in this work for the creation of full-band communication systems in order to satisfy the demands of upcoming high-speed, high-bandwidth data transmission requirements.

Keywords: praseodymium-erbium co-doped fiber amplifiers, full-band, fiber optic communication.

1. Introduction

Along with the continuously developing of optical fiber communication systems, there is a growing demand for broadband high-speed communication systems and high-quality signal transmission. Currently, conventional erbium-doped fiber optic systems operate in the 1500 to 1600 nm transmission window, with single-channel rates exceeding 1 Tb/s, but the wavelength range covers only the C- and L- bands, and there are still many bands that are less used. Information transmission across a wider range of wavelengths is much more crucial because there isn't much space for progress in electronics due to bottlenecks. To be able to transport information over great distances in a larger variety of wavelengths without distorting the information, the design of fiber optic light sources has become essential.

In addition to rare-earth ions such as erbium (Er^{3+}), activated bismuth has also been extensively studied, and the feasibility of bismuth-doped optical fiber amplification was demonstrated in 2001 by Y. Fujimoto et al., who used 800 nm lasers to pump bismuth-doped glass to achieve optical amplification near 1.3 μm [1]. Later doping of metallic elements was extended to include transition metal (TM) and other heavy metal (HM) ions, such as lead and vanadium [2-4]. Co-doping schemes, in addition to single-element doping, have also been proved to be one of the crucial ways to increase the transmission window. For example, the bismuth-erbium co-doped optical fiber has an ultra-broadband emission in the range of 1000 to 1570 nm, which includes various optical bands, allowing a significant expansion of the operating bands [5]. Rare earth (RE) co-doped systems, however, have received very little attention from researchers despite being crucial components of optical amplifiers and laser sources in telecommunication systems [6]. This paper uses a praseodymium-erbium (Pr^{3+}-Er^{3+}) co-doping scheme is used to achieve ultra-broadband luminescence.

Pr^{3+} ions have a wide gain bandwidth and are considered to be a very promising material for amplifiers [7]. In this paper, we will model the signals of the four-energy and three-energy systems of Pr^{3+} and Er^{3+} ions, respectively, to research the layout and optimization of praseodymium-erbium (Pr^{3+}-Er^{3+}) co-doping for full-band fiber-optic amplifiers. Furthermore, to enhance the gain and power

of the co-doped praseodymium-erbium (Pr^{3+}-Er^{3+}) fiber amplifier, we also intend to optimize the structural and parametric layout of the amplifier, including the fiber length and the concentration of doped ions. We will use MATLAB software program to evaluate and optimize different parameter combinations to determine the best amplifier design.

2. Literature Review

Next, we will focus on a literature review and analysis of four of the papers we referenced.

In this paper [2], we demonstrate the synthesis of praseodymium doped fluorotellurite, and detected a wide-band photoluminescence (PL) spanning a wavelength from 1.30 to 1.67μm at 488nm and 590 wavelength excitations. Given its plentiful multi-energy levels, Pr^{3+} among the rare earth ions exhibits the ability to create luminescence in certain infrared bands within an extended low-energy window. Moreover, the near-infrared PL spectra of the Pr^{3+} doped specimens under the conditions of 488 nm are also presented. First, PL intensity rises for samples with low Pr^{3+} doping concentration. The emission peak moves to the short wavelength side as Pr^{3+} levels rise, while the emission band narrows on the long wavelength side. The photoluminescence excitation spectrum (PLE) is measured at 1480nm, and a wide excitation band extending from 440nm to 490nm also contributes to the near infrared emission. The 488nm and 1480nm in the paper are the same wavelengths required in our current study.

Tm^{3+} -doped tellurite glass is studied as the main body of 1.47μm broadband amplifier to extend the fiber transmission bandwidth to Er^{3+}-doped fiber amplifier in this paper [8]. The tellurite erbium-doped fiber amplifier (EDFA) module offers a flat gain of more than 76 nm at the wavelengths 1532~1608 nm, whereas the fluoride TDFA module offers an extra gain of 37 nm at the wavelengths 1443~1484 nm, as can be observed from this study. The gain bands of the two module amplifier modules are separated by 48 nm. The tellurite body's half-height width is 114 nm, while that of ZBLAN is 76 nm. The tellurite glass's numerous doping sites, which also result in a broad Er^{3+} fluorescence and a Tm^{3+} emission peak redshift of around 6 mm to 1468 nm in the tellurite glass and a Tm's emission anomaly of 1462 nm in ZBLAN, may be the cause of the widening. Tm^{3+} - and Er^{3+} -tellurite cross each other at 1510 nm, which is below the shoulder of Er^{3+}. The Tm^{3+} and Er^{3+} -tellurite spectra are crossed at a shorter wavelength of 1495 nm. This allows us to take advantage of the 1470 nm experimental data.

In order to increase the bandwidth and the quantum efficiency of the fiber, a new near-infrared emission can be obtained by using praseodymium [9]. But at the same time, it is impossible to observe the absorption spectrum because of the fact that H and F are strongly absorbed at the long end of the wavelength. Therefore, the scheme of praseodymium-erbium co-doped (Pr^{3+}-Er^{3+}) is proposed to realize ultra-wideband near-infrared emission. Under the excitation of 488nm, erbium ions' effective emission/amplification has been proved. The standard gallium erbium co-precipitation sample was obtained according to the quenching procedure. By analyzing the absorption spectrum of the praseodymium-erbium co-doped sample at room temperature, the respective excitation spectra of the praseodymium and the erbium element and the absorption spectrum of the joint action are observed. The results show that the absorption band of single- doped praseodymium ions is caused by the transfer of the electron from the ground to the corresponding excited states. In addition, we can find out from the diagram that praseodymium is able to efficiently pump the blue light source. Notably, there are identical absorption peaks between praseodymium and erbium ions. This resonance energy level matching makes it possible for praseodymium-erbium co-doped to achieve ultra-wideband emission, consistent with the excitation spectrum.

This paper uses spectrophotometry to analyze the rare earth element praseodymium, mainly examines the absorption spectrometry of solutions with a concentration of 0.037~37 mg/ml, and uses spectrophotometry to make relatively fine measurements of solutions with lower concentrations [10]. Furthermore, the effects of the concentration, the base point and the standard solution on the micro-spectral properties of praseodymium have been studied. It is found that the concentration of

praseodymium in the range of 0.037mg/ml to 0.37mg/ml can be precisely measured by the absorption spectrum. When the influence of concentration on the absorption spectrum is investigated in the article, as the longitudinal coordinates of the absorption spectrum are gradually reduced from 4.0 to 0.07, the characteristic absorption peaks of the gallium will gradually appear from the original straight line (when the absorption peak is a straight line, it is basically impossible to be accurately measured). They all have high availability, and all of them have high availability. The test results show that when the concentration is 37 mgPr/ml, the absorption spectrum characteristics, which is a straight line, are not obvious. However, as the concentration decreases, the range of change of the baseline shape of the praseodymium absorption spectrum gradually increases, and the baseline peak is gradually formed. From this, it is observed that the valuable spectral absorption peak is 444nm. The working wavelength required for the research is roughly the same.

3. Models and Methods

3.1. Energy level system selection

In praseodymium-erbium (Pr^{3+}-Er^{3+}) co-doped fiber amplifiers, erbium ions (Er^{3+}) are in a three-energy level system while praseodymium ions (Pr^{3+}) are in a four-energy level system. These fiber amplifiers may function at wavelengths of 1300 to 1650 nm. The two components of four- and three-energy level systems will be discussed individually in the following sections.

3.1.1. Four-energy level system

This paper will focus on the four-level structure of praseodymium ions. The energy level E_1 is the ground state, the energy level E_2 and E_3 are the lasing upper energy level and the lower one, collectively known as the sub-stable state, and the energy level E_4 is the excited state. A pumping mechanism is initially used to move the particles from the lower energy level of the ground state to the higher energy level. After a short time period τ_{32}, the particles are transferred to the upper energy level of the laser in a non-radiation transition. The particles can be transported from the upper- to the lower laser energy level by both spontaneous and stimulated radiation, and the duration of the transport process is τ_{21}. Finally, the particles return to the ground state energy level in a non-radiative manner in a short time period of τ_{10}.

Four-energy level rate equations:

$$\frac{\partial N_1(z)}{\partial t} = -W_p(z)N_1(z) + A_{21}N_2(z) \tag{1}$$

$$\frac{\partial N_2(z)}{\partial t} = A_{12}(z)N_z(z) - W_{23}(z)N_2(z) + W_{32}N_3(z) + A_{32}N_3(z) \tag{2}$$

$$\frac{\partial N_3(z)}{\partial t} = W_{23}(z)N_2(z) - W_{32}(z)N_3(z) - A_{32}N_3(z) + A_{43}N_4(z) \tag{3}$$

$$\frac{\partial N_3(z)}{\partial t} = W_p(z)N_1(z) - A_{32}N_3(z) \tag{4}$$

$$N = N_1(z) + N_2(z) + N_3(z) + N_4(z) \tag{5}$$

$$N1 = \frac{A_{21}A_{32}A_{43}N + A_{21}A_{43}NW_{32}}{A_{21}A_{32}A_{43} + A_{21}A_{43}W_{32} + A_{21}A_{32}W_P + A_{21}A_{43}W_P + A_{32}A_{43}W_P + A_{21}W_{32}W_P + A_{43}W_{23}W_P + A_{43}W_{32}W_P} \tag{6}$$

$$N2 = \frac{A_{43}NW_P(A_{32} + W_{32})}{A_{21}A_{32}A_{43} + A_{21}A_{43}W_{32} + A_{21}A_{32}W_P + A_{21}A_{43}W_P + A_{32}A_{43}W_P + A_{21}W_{32}W_P + A_{43}W_{23}W_P + A_{43}W_{32}W_P} \tag{7}$$

$$N3 = \frac{A_{43}NW_P(A_{21} + W_{32})}{A_{21}A_{32}A_{43} + A_{21}A_{43}W_{32} + A_{21}A_{32}W_P + A_{21}A_{43}W_P + A_{32}A_{43}W_P + A_{21}W_{32}W_P + A_{43}W_{23}W_P + A_{43}W_{32}W_P} \tag{8}$$

$$N4 = \frac{NW_P(A_{21}A_{32}+A_{21}W_{32})}{A_{21}A_{32}A_{43}+A_{21}A_{43}W_{32}+A_{21}A_{32}W_P+A_{21}A_{43}W_P+A_{32}A_{43}W_P+A_{21}W_{32}W_P+A_{43}W_{23}W_P+A_{43}W_{32}W_P} \quad (9)$$

All the parameters in the equations are summarized in the following Table 1.

Table 1. Description of the parameters of the four-energy rate equation

Parameter	Parameter description
W_P	Pump light absorption rate
W_{12}	Signal light absorption rate
W_{21}	Signal light stimulated emission rate
A_{32}	Radiative excitation rate
A_{21}	Non-radiation transition rate
A_{43}	Non-radiation transition rate
N_1	Particle number density in E_1 energy level
N_2	Particle number density in E_2 energy level
N_3	Particle number density in E_3 energy level
N_4	Particle number density in E_4 energy level
N	Total particle number density

Four-energy level power propagation equations:

$$\frac{dP_p(z)}{dz} = -\Gamma_p(\sigma_p N_1(z) + \alpha_a)P_P(z) \quad (10)$$

$$\frac{dP_s(z)}{dz} = \Gamma_s[\sigma_{32}N_3(z) - \sigma_{23}N_2(z) - \alpha_s]P_s(z) \quad (11)$$

$$\pm\frac{dP_{ase}(z)}{dz} = \pm\Gamma_{ase}[\sigma_{32}N_3(z) - \sigma_{23}N_2(z) - \alpha_s]P_s(z) \pm 2\sigma_{32}N_3(z)h\upsilon\,\Delta\upsilon \quad (12)$$

All the parameters in the equations are summarized in the following Table 2.

Table 2. Description of the parameters of the four-energy level power propagation equation

Parameter	Parameter description
P_p	Pump power
P_S	Signal power
P_{ase}	ASE
α	Loss factor of fiber material
$\Delta\upsilon$	Full width at half maximum of frequency
Γ_p	Pump light overlap integration factor
Γ_s	Signal light overlap integration factor
Γ_{ase}	Overlap integration factor for spontaneous radiation
σ_p	Pump light absorption cross section
σ_{32}	Signal light emission cross section
σ_{23}	Signal light absorption cross section

3.1.2. Three-energy level system

The particles in the ground state energy level E_1 in the three-level system absorb pump light energy before transiting to the high energy level E_3, whereas the particles in the E_3 energy level will be rapidly transferred to the sub-stable E_2 energy level by non-radiation transition. The ground state energy level particles continue to transit to the E_2 energy level under the influence of the pump source because of the long lifetime of E_2 particles. As a result, the quantity of particles in the E_2 energy level will continue to accumulate until it realizes the population inversion between energy levels E_2 and E_1.

It is necessary to form such a cycle for efficient amplifier amplification of the signal light. Figure 1 illustrates the three-energy structure of the thulium ion.

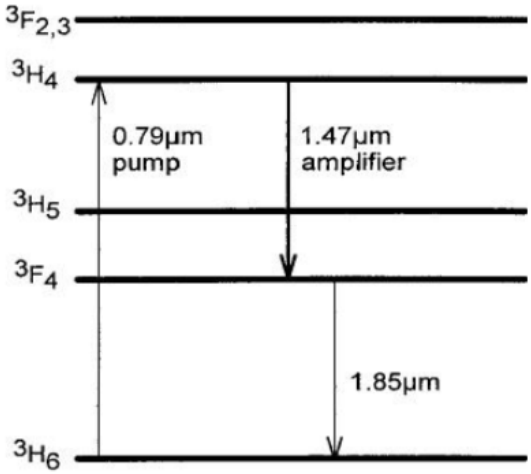


Figure 1. Structure of the three energy levels system [8]

Three-energy level rate equations:

$$\frac{\partial N_1(z)}{\partial t} = -[W_p(z) + W_{12}(z)]N_1(z) + A_{21}N_2(z) + W_{21}N_2(z) \tag{13}$$

$$\frac{\partial N_2(z)}{\partial t} = W_{12}(z)N_1(z) - W_{21}N_2(z) - A_{21}N_2(z) + A_{32}(z)N_3(z) \tag{14}$$

$$\frac{\partial N_3(z)}{\partial t} = W_p(z)N_1(z) - A_{32}N_3(z) \tag{15}$$

$$N = N_1(z) + N_2(z) + N_3(z) \tag{16}$$

Three-energy level power propagation equations:

$$\frac{dP_p(z)}{dz} = -\Gamma_p(\sigma_p N_1(z) + \alpha_a)P_P(z) \tag{17}$$

$$\frac{dP_s(z)}{dz} = \Gamma_s[\sigma_{21}N_2(z) - \sigma_{12}N_1(z) - \alpha_s]P_s(z) \tag{18}$$

3.2. Design of parameter:

In the parameter design part, we use Pr^{3+}, whose working wavelength range is in L+ band as an example for detailed analysis. We can observe from the below Figure 2 that Pr^{3+}, which belongs to a four-energy level system, has a wavelength range that can accommodate the L+ band when the center wavelength of the signal stimulated emission is 1490 nm. We take the central wavelength of the signal light 1625 nm for example. When being pumped with a wavelength of 488 nm, the signal light will produce excited emission, which transits from the $^1D_2$ to the $^1G_4$ energy level, satisfying the four-energy system required for praseodymium-doped fiber amplifiers. In addition, we were surprised to find that both Pr^{3+} and Er^{3+} could be transited at the pump light wavelength of 488 nm.

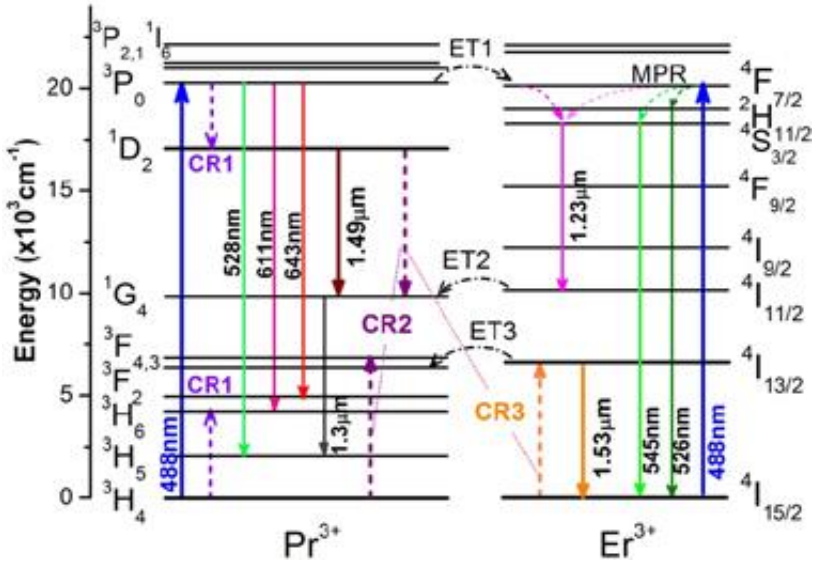


Figure 2. Graph of the energy levels of Pr^{3+} and Er^{3+} [9]

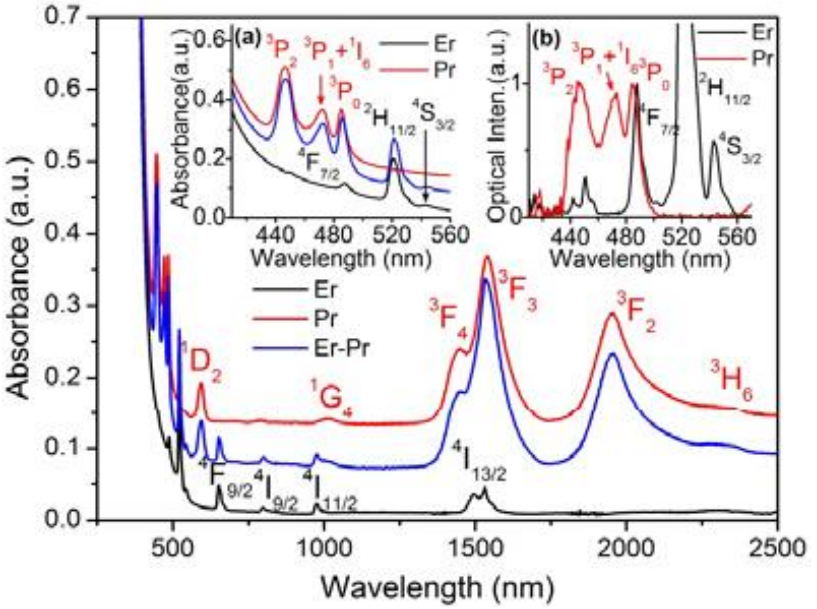


Figure 3. Absorbance spectra of Pr^{3+}-, Er^{3+}- single-doped and Pr^{3+} -Er^{3+} co-doped samples [9]

In a case when the pump light has a wavelength of 488 nm and the signal light's wavelength is 1625 nm, through reviewing the references [10], according to Figure 3, it can be calculated that in the praseodymium-doped fiber amplifier, the pump light's absorption cross section is $\sigma_p = 0.89 \times 10^{-24} m^2$. The signal light's emission cross section is $\sigma_{32} = 3 \times 10^{-24} \mathrm{m}^2$.

The absorption cross section of signal light can be calculated from its emission cross section σ_{23}:

$$v = c \times le9/1625 \tag{19}$$

$$\sigma_{23}(v) = \sigma_{32}(v)\, exp(\frac{\varepsilon_0 - hv}{KT}) \tag{20}$$

The absorption cross section is calculated as:

$$\sigma_{23} \approx 3 \times 10^{-24} m^2 \tag{21}$$

So far, we have obtained all the parameters required for the four-energy level system of praseodymium-doped fiber amplifier with the pump light's wavelength of 488 nm and the signal light's wavelength of 1625 nm. Then we substitute the values into the rate and the power propagation equation. Using MATLAB to solve numerically, the gain spectrum is programmed to vary with the fiber length and doping concentration, and the maximum gain of the signal is attained at what the fiber length and dopant ion concentration are respectively.

4. Results and discussion

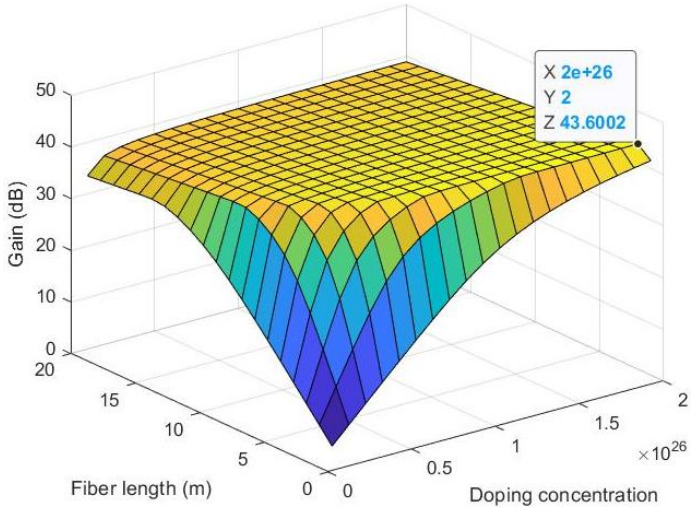


Figure 4. Operational result of praseodymium-doped fiber-optic amplifier at 1625 nm wavelength

After running the program, we are able to see the variation of gain (dB) with ion doping concentration (ions/m^2) and fiber length (m) in a three-dimensional graph, as shown in Figure 4. We set the fiber length variation range interval to 1 (m) and the ion doping concentration variation range interval to 1×10^{25} (ions/m^2). We may conclude from the figure that the overall gain of the fiber amplifier can be increased by either ion doping concentration or fiber length. When the length of the optical fiber is constant, the gain increases positively with the ion doping concentration; while when the ion doping concentration is constant, the gain tends to increase with the length of the optical fiber, showing a tendency to increase rapidly at first, and then declines slowly after reaching its peak value. The gain of the optical fiber amplifier achieves the maximum value, which is 43.6002 (dB), when the optical fiber has a length of 2 (m) and the doping concentration of 2×10^{26} (ions/m^2).

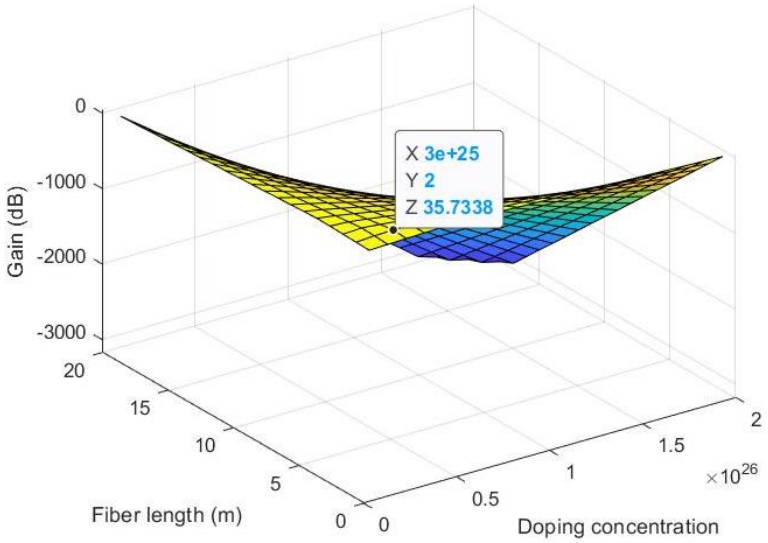


Figure 5. Operational result of erbium-doped fiber-optic amplifier at 1470 nm wavelength

Similarly, we can plot a three-dimensional graph of the EDFA at 1470 nm, as shown in Figure 5. The variation range interval of the fiber length and the variation range interval of the ion doping concentration are set to be the same as above. We can find that the ion doping concentration and fiber length substantially impact the fiber amplifier's gain at this time, causing a very significant change. When the fiber length is constant, the gain increases gradually with the increase of ion doping concentration, and then decreases rapidly once it reaches the extreme value, and the rate of gain decrease is positively correlated with the fiber length; while when the ion doping concentration is unchanged, the trend of the gain with the fiber length is the same as the trend of the gain with the change of ion doping concentration. At the fiber length of 2 (m) and the doping concentration of 3×10^{25} (ions/m^2), the fiber amplifier gain reaches the maximum, which is 35.7338 (dB).

Simulated annealing algorithm

However, since this method is time-consuming and not accurate enough, we will additionally use the simulated annealing algorithm method to optimize the fiber length and doping concentration of praseodymium- and erbium-doped fiber amplifier models in order to maximize the peak gain in this paper, and to verify the accuracy of the previous three-dimensional graphs.

Simulated annealing algorithm is a stochastic optimization method that simulates the annealing process in a thermodynamic system [11]. Annealing is the process of heating a substance above its melting point and cooling it to form a crystal structure. In the algorithm, there are several different atom states, each of which corresponds to a different energy. In this method, an object function is considered as the energy of all states in the system, and then a solid state is found, which is equivalent to the global optimum solution. This approach is effective in preventing the problem from falling into the local optimum because the present solution has a probability to be replaced by the new solution in each iteration.

The results obtained are as follows:

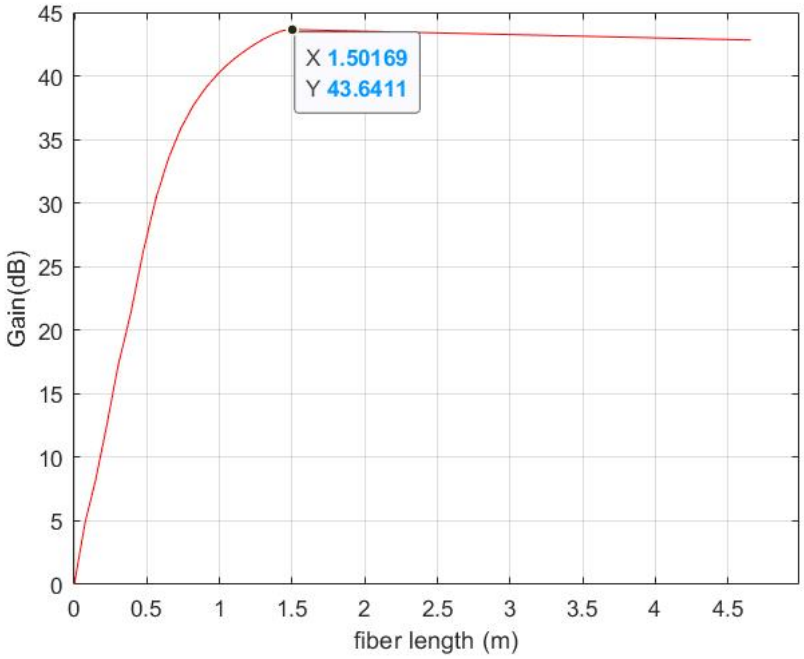


Figure 6. Optimization result of praseodymium-doped fiber amplifier

From Figure 6, we can discover that when the fiber length is less than 1.502 (m), there is a positive increase in the fiber amplifier's gain along with the fiber length at a gradually decreasing slope. The amplifier gain stops changing or starts to steadily decline with fiber length after exceeding 1.502 meters. The PDFA has a maximum gain of 43.64 (dB) when the fiber length L is 1.502 (m) and the ion concentration is 1.81722×10^{26} (ions/m^2), which is mostly compatible with the outcomes of the three-dimensional diagram in the main program.

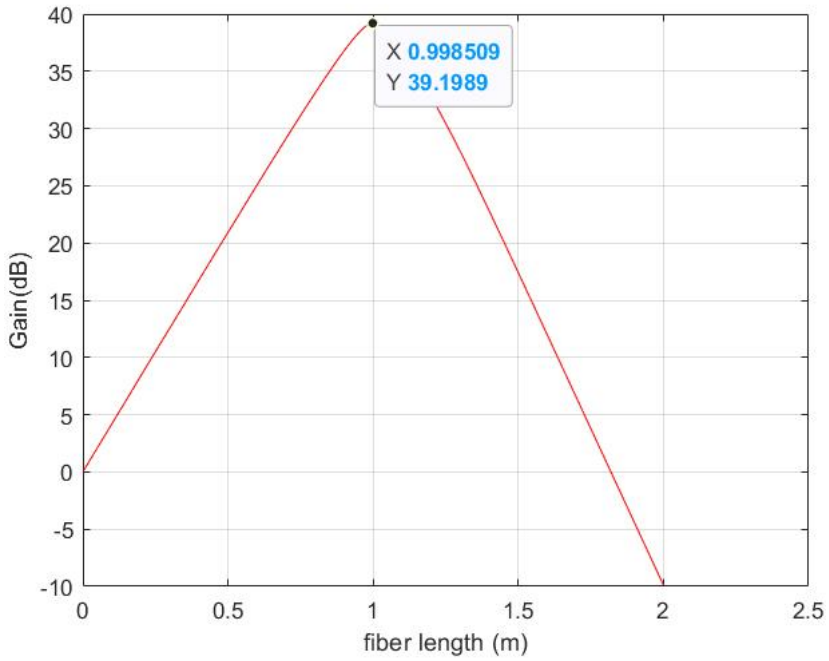


Figure 7. Optimization result of erbium-doped fiber amplifier

Figure 7 shows that when the fiber length is less than 1 (m), the amplifier's gain increases positively with the fiber length, resembles a main function virtually, and reaches its peak value at the 1m fiber length. The amplifier gain rapidly declines with fiber length when it is longer than 1 (m). The maximum gain of the EDFA is 39.1989 (dB), when the fiber length L is 1 (m) and the ion concentration is 5.7665×10^{25} (ions/m^2), which is basically consistent with the trend of the three-dimensional diagram in the main program.

5. Conclusion

In this study, we have designed a full-wave band with a pump light of 488 nm and a power of 200 mW, investigate and analyze the spectral properties of praseodymium ions (Pr^{3+}) and erbium ions (Er^{3+}) and their corresponding energy level structures, establish the rate equations and power propagation equations of the fiber amplifiers, and ultimately obtain the curves of the praseodymium-doped and erbium-doped optical fiber gains with the ion doping concentration and the length of the fibers, respectively. In addition, simulated annealing algorithm is used to optimize the structure of the established praseodymium and erbium co-doped fiber amplifiers.

This experiment illustrates that when the fiber length is 2.479 (m) and the ion concentration is 1.81×10^{26} (ions/m^2), the signal gain in the praseodymium-doped fiber amplifier achieves its maximum value of 44.242 (dB). And in the erbium-doped fiber amplifier, the signal gain reaches the biggest data of 39.1989 (dB) when the fiber length is 1 (m) and the ion concentration is 5.7665×10^{25} (ions/m^2).

However, there are certain flaws in the experiment itself. For instance, we have taken only specific bands of praseodymium and erbium doped ion fiber amplifiers, so the experimental data is not generalized sufficient in terms of the points used. In addition, the interval range of the sampled points in the three-dimensional model is all in one minimum unit, which results in discrete spots in the figure and inaccurate values. Due to the simulated annealing algorithm's short iteration time, numerical mistakes can be made.

Authors Contribution

All the authors contributed equally and their names were listed in alphabetical order.

References

[1] M. Peng, J. Qiu, D. Chen, X. Meng, and C. Zhu. Superbroadband 1310 nm emission from bismuth and tantalum codoped germanium oxide glasses. Opt. Lett. 30 (18), 2433 - 2435 (2005).

[2] Zhou, Bo, et al. Superbroadband near-IR photoluminescence from Pr 3+-doped fluor tellurite glasses. Optics express 20.4, 3803 - 3813 (2012).

[3] Cheng, C., Wang, F., & Cheng, X. Pbse quantum-dot-doped broadband fiber amplifier based on sodium-aluminum-borosilicate-silicate glass. Optics & Laser Technology, 122, 105812 (2020).

[4] Hughes, M., Curry, R. J., Rutt, H., & Hewak, D. Spectroscopy of vanadium (III) doped gallium lanthanum sulphide chalcogenide glass. 10.1063/1.2432280 (2014).

[5] Yanhua Luo, Jianxiang Wen, Jianzhong Zhang, John Canning, and Gang-Ding Peng. Bismuth and erbium codoped optical fiber with ultrabroadband luminescence across O-, E-, S-, C-, and L-bands. Opt. Lett. 37, 3447 - 3449 (2012).

[6] M. J. F. Digonnet. Rare-Earth-Doped Fiber Lasers and Amplifiers. Marcel Dekker, (2009).

[7] Liang, X. W., & Huang, S. B. 1.3μm band praseodymium-doped fiber amplifier [J]. Neijiang Science and Technology, 30 (09): 74+144 (2009).

[8] Sx., N. M. J. A. S. Tm3+-doped tellurite glass for a broadband amplifier at 1.47 mu m. Applied optics, 39 (27) (2000).

[9] Zhou, B., Tao, L., Tsang, Y. H., Jin, W., & Pun, Y. B. Superbroadband near-infrared emission and energy transfer in pr3+-er3+ codoped fluorotellurite glasses. Optics Express, 20 (11), 12205 - 12211 (2012).

[10] Sun Ducheng, Peng Yang, Guan Xiaomei et al. Study and application of fine absorption spectra of praseodymium hydrochloride solution [J]. Journal of Xinjiang University (Natural Science Edition), 1998 (03): 50 - 53.

[11] Qu Qiang, Chen Xuebo. Implementation of simulated annealing algorithm based on MATLAB [J]. Journal of Anshan University of Science and Technology, 2003 (03): 196 - 199.